Asociación Argentina
de Mecánica Computacional

Mecánica Computacional Vol XXIX, págs. 8411-8420 (artículo completo)
Eduardo Dvorkin, Marcela Goldschmit, Mario Storti (Eds.)
Buenos Aires, Argentina, 15-18 Noviembre 2010

DESIGN OF SPARK PLASMA SINTERING GRAPHITE DIE USING TOPOLOGY OPTIMIZATION

Flávio M. Vasconcelos, Luis A.M. Mello and Emílio C. N. Silva

Department of Mechatronics and Mechanical Systems Engineering, Escola Politécnica da Universidade de São Paulo, Avenida Prof. Luciano Gualberto, travessa 3 n° 380, São Paulo, Brasil, pos.grad@poli.usp.br, http://www.poli.usp.br

Keywords: Topology Optimization, Spark Plasma Sintering, Temperature distribution, Graphite Die.

Abstract.

The Spark Plasma Sintering (SPS) is a sintering process which uses a graphite die and punchers in its tool system. This technique has been employed to sinter a large number of materials, especially Functionally Graded Material (FGM), in which the material gradation, in some cases, requires a temperature gradient in the sample region during the manufacturing process to ensure uniform sintering. An optimized die design that generates a temperature gradient can be developed by changing the die wall thickness. However, this design presents some difficulties because it deals with bidimensional problems subject to convection and radiation heat transfer boundary conditions, and with conductive and/or non-conductive FGM sample. Thus, in this work, the Topology Optimization Method (TOM) is applied to design a graphite die to achieve a predefined temperature gradient. The TOM is able to provide an optimum topology for the die by seeking a material distribution inside a given domain that extremizes a cost function and satisfies the constraints of the optimization problem. In order to simulate the SPS process, a electrical-thermal coupled steady state problem is modeled using finite element formulation based on the governing equations. In the developed model, the convective heat transfer is neglected once the process takes place in vacuum, the radiation process is linearized to reduce the modeling complexity, and the properties of the graphite and sample are assumed not to depend on temperature. In the topology optimization problem the temperature gradient is established through a cost function that minimizes the difference between the prescribed gradient and the calculated temperature subjected to a material volume constraint. Results of optimized graphite dies are presented.

1 INTRODUCTION

The Spark Plasma Sintering (SPS) is a powder consolidating and sintering process which uses pulse DC current and pressure loads that are applied simultaneously to the die components (electrodes, spacers, punchers and graphite die). The powders are placed in the graphite die and, while the pressure load transmitted by the punchers carries out the densification, a pulse DC current flows through the die and sample (in case of conductive sample) providing a high heating rate and promoting the sinterization. A schematic representation of the SPS process is shown in Figure 1.

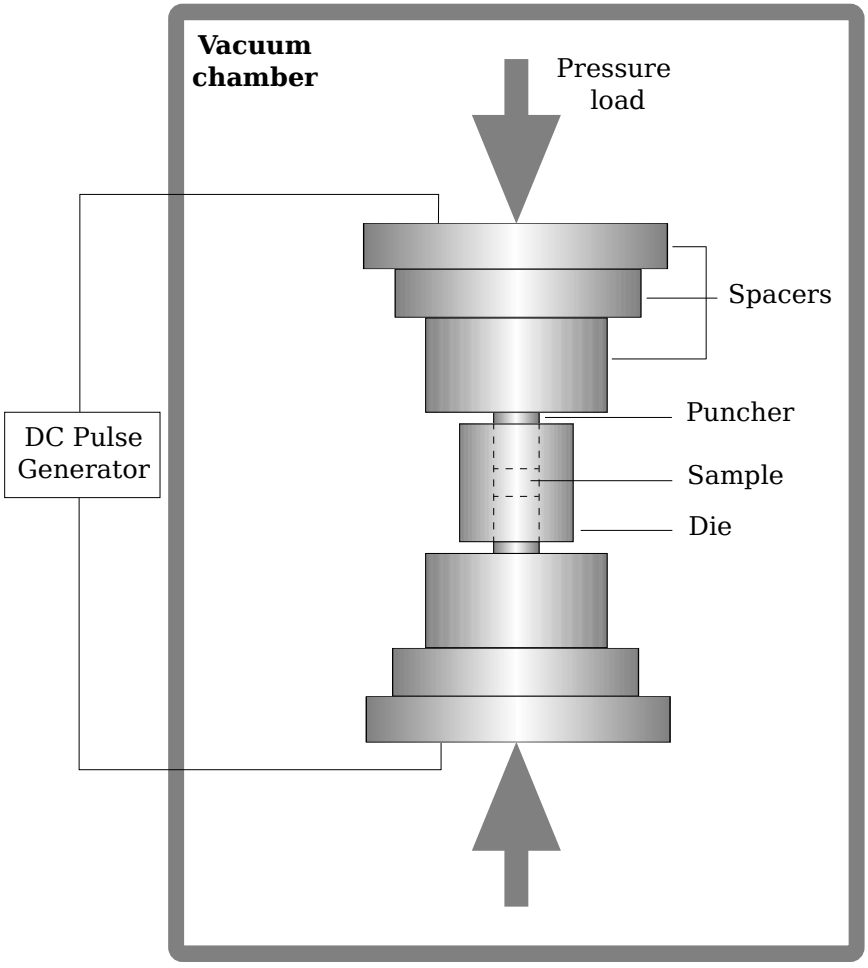

Figure 1: SPS process schematic representation.

There has been some work regarding the current and temperature distribution of the SPS process. Yucheng and Zhengyi (2002) used analytical solutions in the one-dimensional case to calculate the temperature difference between die and sample. Zavaliangos et al. (2004) perfomed electrical-thermal analysis using commercial package considering the contact resistances. Anselmi-Tamburini et al. (2005) investigated the effects of sample conductivities on the current and temperature distributions. Vanmeensen et al. (2005) also presented results concerning the sample material properties. Wang et al. (2007) studied the influence of material and control parameters on the electrical-thermal-mechanical coupled problem given informa-

tion about thermal and stress distribution. The latest study reported in the literature carried out by Tiwari et al. (2009) investigated a fully electrical-thermal coupled problem with finite element analysis and varying the sample conductivity and different power input. For the most part, the results presented show a reduced temperature gradient in the sample region in both radial and axial direction.

The SPS method has been employed to sinter a large number of materials, especially Functionally Graded Material (FGM), in which the material properties change gradually with position. This material gradation, in some cases, requires a temperature gradient in the sample region during the manufacturing process to ensure uniform sintering. Therefore, the die can be optimized in order to meet the mentioned requirement. However, this design presents some difficulties because it deals with a bidimensional problem subject to convection and radiation heat transfer boundary conditions.

Optimization problems that consider thermal boundary conditions have been discussed. To deal with this type of problem, effective methodologies have been proposed. Bruns (2007) carried out experiments, focusing on the numerical instabilities that can severely affect the optimization and describing a method to avoid such instabilities. Gao et al. (2008) studied a steady state heat conduction problem under both design-independent and design-dependent loads by modified bidirectional evolutionary structural optimization. Iga et al. (2009) performed several numerical examples that focus on design-dependent effects related to heat convection and internal heat generation for optimal designs, in which a method to extract the structural boundaries for heat convection loads is proposed.

Based on these studies, the Topology Optimization Method (TOM) is proposed to design graphite die with a predefined temperature gradient. The TOM is able to provide an optimum topology for the die by seeking a material distribution inside a given domain that extremizes a cost function and satisfies the constraints of the optimization problem. In order to simulate the SPS process, an electrical-thermal coupled steady-state problem is solved by using a model based on the Finite Element Method (FEM). In this model, the convective heat transfer that may occur in the vacuum chamber is neglected and the radiation process is linearized to reduce the model complexity. We also use design-dependent loads due to the changes of the die geometry during the optimization process that affects the thermal loads. This thermal load consists of the heat generation due to joule heating and radiation between the free surfaces of all die components in the vacuum chamber.

This paper is organized as follows. In Section 2, the FEM-based computational model is presented. In Section 3, the solution of the optimization problem is discussed. In Section 4, results are presented and concluding remarks are provided in Section 5.

2 FINITE ELEMENT FORMULATION

A linear and two-dimensional steady-state electrical-thermal coupled problem is considered in order to reduce complexity and computational cost. The electrical potential and temperature distributions in the die (see Figure 2) are obtained based on the set of governing partial differential equations (PDE's):

$$\nabla \cdot \vec{J} = 0 \tag{1}$$

$$\nabla \cdot (-k\nabla T) = \dot{q} \tag{2}$$

where $\vec{J} = \sigma\vec{E}$ is the current density, $\vec{E}$ is the electrical field and σ is the eletrical conductivity.

The term $-k\nabla T$ is the heat flux density with k being the thermal conductivity and $\dot{q} = \vec{J} \cdot \vec{E} = |\vec{J}||\vec{E}| = JE$ the internal heat generation per unit volume.

The finite element formulation is based on the integral form of equations 1 and 2. The equilibrium equations can be expressed as

$$\int_{\Omega} \nabla \tilde{V} \mathbf{C_e} \nabla V \mathrm{d}\Omega = 0 \tag{3}$$

$$\int_{\Omega} \nabla \tilde{T} \mathbf{C_t} \nabla T \mathrm{d}\Omega - \int_{\Gamma} \tilde{T} \mathbf{C_t} \frac{\partial T}{\partial n} \mathrm{d}\Gamma + \int_{\Omega} \dot{q} \tilde{T} \mathrm{d}\Omega = 0 \tag{4}$$

where V is the electrical potential field and T is the temperature field, and $\tilde{V}$ and $\tilde{T}$ are the corresponding virtual fields. Ω is the domain with boundary Γ, and $\mathbf{C_e}$ and $\mathbf{C_t}$ are the electrical and thermal conduction tensors, respectively.

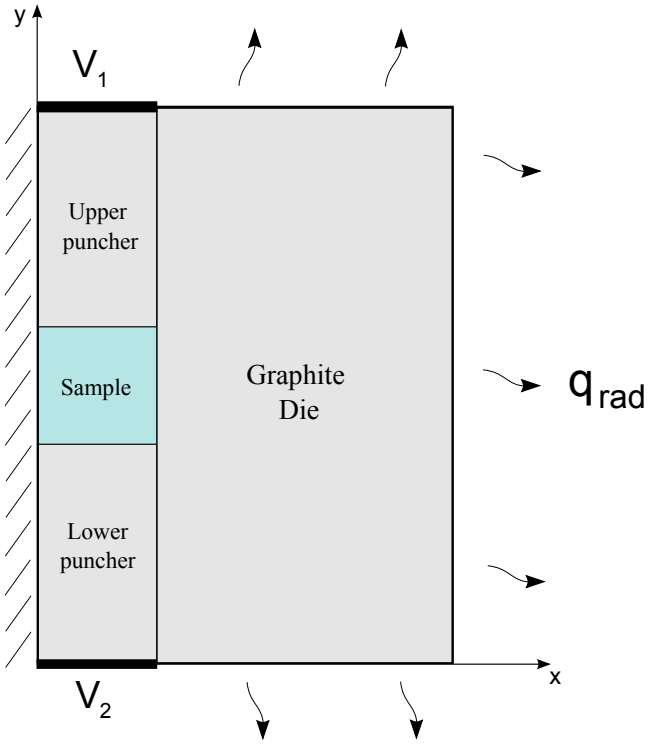

Figure 2: Electrical-thermal coupled problem model.

In order to simulate the SPS process, a two-dimensional model with unitary thickness is developed as shown in Figure 2. In this model, the electrical problem has its boundary conditions as an electrical potential V_1 and V_2 prescribed at the top of the upper punch and at the bottom of the lower punch, respectively. For the thermal problem, the heat transfer boundary conditions are given by the radiation between the graphite die free surfaces and the vacuum chamber interior. Here, the radiation term q_{rad} is linearized and given as

$$q_{rad} = \varepsilon\kappa({T_w}^4 - {T_{surr}}^4) \approx q_0 + \left.\frac{\partial q}{\partial T}\right|_{T_0} (T - T_0) \tag{5}$$

where the emissivity ε is assumed to be equal to 1, κ is the Stefan-Boltzmann constant, T_w is the temperature of the die surface, T_{surr} is the temperature in the vacuum chamber and q_0 is the energy radiation evaluated at the linearization temperature T_0. Therefore, the linearized radiation (equation 5) can be interpreted as a prescribed heat flux and an apparent convective heat flux in the FE formulation.

After discretization (four nodes isoparametric elements are used), the equilibrium equations can be rewritten in the matrix form as

$$\mathbf{K}_e \mathbf{U}_e = 0 \tag{6}$$

$$\mathbf{K}_t \mathbf{U}_t = \mathbf{F}_t \tag{7}$$

Subscripts e and t are related to the electrical and thermal problems, respectively. $\mathbf{K}$ is the conductivity matrix, $\mathbf{U}$ is the nodal solution vector, and $\mathbf{F_t}$ is the load vector. Using the thermal boundary conditions, the conductivity matrix and the load vector are

$$\mathbf{K}_t = \mathbf{K}_k + \mathbf{K}_{hb} \tag{8}$$

$$\mathbf{F}_t = \mathbf{F}_{\dot{q}} + \mathbf{F}_{q_0} + \mathbf{F}_{hb} \tag{9}$$

where $\mathbf{K}_k$, $\mathbf{K}_{hb}$, $\mathbf{F}_{\dot{q}}$, $\mathbf{F}_{q_0}$ and $\mathbf{F}_{hb}$ are the thermal conduction matrix, heat transfer matrix, internal heat generation vector, heat flux vector and heat transfer vector, respectively.

3 FORMULATION OF TOPOLOGY OPTIMIZATION

The Topology Optimization (TO) consists of a material distribution problem based on a fixed domain D that includes the original design. The characteristic function of TO can be stated as follows:

$$\chi_\Omega = \begin{cases} 1 & \text{if} \quad \mathbf{x} \in \Omega_d \\ 0 & \text{if} \quad \mathbf{x} \in D \setminus \Omega_d \end{cases} \tag{10}$$

where $\mathbf{x}$ denotes the position in the fixed design domain D and Ω_d is the thermal conductor domain. Since this characteristic function is highly discontinuous, the Solid Isotropic Material Distribution (SIMP) approach is used to carry out the relaxation. This approach can cause numerical instabilities such as checkerboard. To overcome this issue, a Continuous Approximation Material Distribution (CAMD) is assumed and can be expressed as

$$\rho_e = \sum_{i=1}^{m} N_i \rho_i \tag{11}$$

where ρ_e is the distribution function in the element e, N_i is the interpolation functions, ρ_i is the nodal design variable and m is the total number of nodes. The optimization problem is given by:

$$\underset{\rho}{\text{Minimize}} \quad w_1 \mathrm{C}_1 + (1 - w_1)\mathrm{C}_2$$

subject to

$$\mathrm{V} = \int_\Omega \rho \mathrm{d}\Omega \leq \mathrm{V}_{\max}$$
$$\mathbf{K}_t \mathbf{U}_t = \mathbf{F}_t$$
$$0 \leq \rho \leq 1$$

and

$$\mathrm{C}_1 = \sum_{i=1}^{n} (\Delta\Theta_i^j - \alpha)^2 \qquad \mathrm{C}_2 = \mathbf{F_t}^T \mathbf{T} \tag{12}$$

where $\Delta\Theta_i^j = \Theta_{i+1}^j - \Theta_i^j$ is the temperature difference in a specific region j ($j = 1, \ldots, k$) inside the sample and α represents the intended gradient. The term C2 is the mean potential energy and it is used to enforce a discrete (0-1) material distribution in the fixed design domain (please refer to Bendsøe and Sigmund (2003) for an analogous discussion).

Figure 3 shows the discretized sample region and yields the manner in which the temperature gradient is imposed. The w_1 is a penalized weighted factor applied in the objective function and used to guide the optimization and to become the optimization problem well posed.

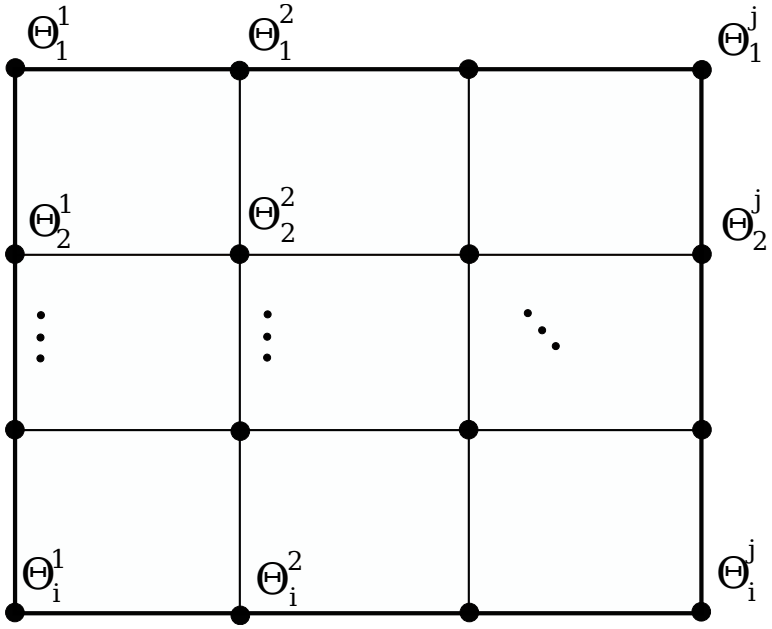

Figure 3: Sample discretization analysis to evaluate the cost function

The optimization problem is solved by using Sequential Linear Programming (SLP) and the gradient of the objective function is obtained through the Finite Difference Method (FDM).

3.1 Formulation of the design-dependent thermal loads

In order to deal appropriately with the thermal boundary conditions during the optimization process, a Hat-function $H(\rho_i, \mathrm{p})$ based on the method proposed by Iga et al. (2009) is used and

illustrated in Figure 4. The Hat-function shown in Figure 4b uses the nodal design variable and a penalization factor p to set the thermal boundary conditions only in the gray scale areas in the fixed design domain, as shown in Figure 4a. The identification of the gray scale areas is carried out by the ρ_{lower} and ρ_{upper} limit values, which in the Figure 4b are equal to 0.2 and 0.8, respectively.

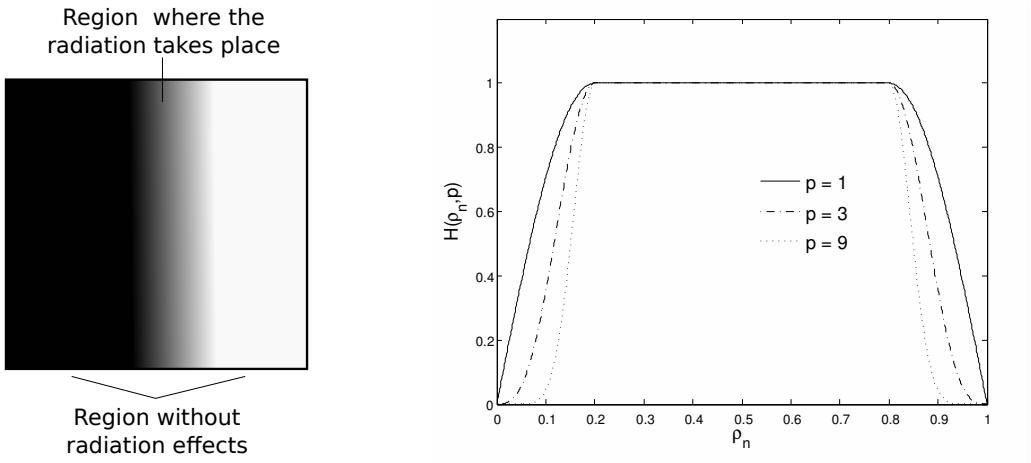

(a) (b)

Figure 4: Modeling to extract structural boundaries for radiation boundaries conditions.

The radiation boundary conditions can then be expressed as

$$q_{rad}(\mathbf{x}) \approx q^r_{rad}(\mathbf{x}) = \sum_{i=1}^{n} N_i H(\rho_i, \mathrm{p}) q_i \tag{13}$$

where q^r_{rad} and q_i stand for the discretized radiation heat transfer and the nodal radiation heat transfer, respectively.

4 PRELIMINARY RESULTS AND DISCUSSION

A finite element (FE) model is developed herein to solve the electrical-thermal coupled problem and implemented using MATLAB code. This model is conducted by employing finite element formulation with four nodes isoparametric elements considering the graphite die, sample and punchers as shown in Figure 2.

In order to set the boundary conditions for the FE model, a numerical simulation is performed using COMSOL Multiphysics considering a graphite sample (with temperature-dependent material properties) and nonlinear thermal radiation heat transfer, to evaluate the electrical potential difference between the upper and lower punchers, and the temperature of the die surface where the radiation takes place. Since the radiation is a highly nonlinear phenomenon, this numerical simulation is necessary to maintain the linearized radiation near the non-linearized one using a linearization temperature as close as possible to the real radiation temperature. The results have shown that the electrical potential difference is about 1 V and the radiation temperature is approximately 1750 K, which is considered as T_0 when the radiation is linearized. In addition, the electrical and thermal interfaces among the punchers, sample and graphite die are modeled in the FE model as continuous, i.e., contact resistances are neglected in this work.

The FE model is used in the optimization algorithm, in which a preliminary sensitivity analysis is performed through FDM and the design variable is updated using SLP. In this model, an isotropic material considered has a 10^5 S/m electrical conductivity and a 50 W/mK thermal conductivity. The temperature T_{surr} surrounding the tool system is set to 300 K and the internal heat generation load is considered a design-independent load. The sample is considered to be made of graphite, as well as the die and punchers. Figure 5 shows the fixed design domain D assumed in the optimization problem and illustrated the manner of how the domain discretization is performed using 10x16 rectangular elements. The initial configuration of the fixed design domain has a uniform design variable distribution equal to 0.75 and the V_{max} is equal to 60%.

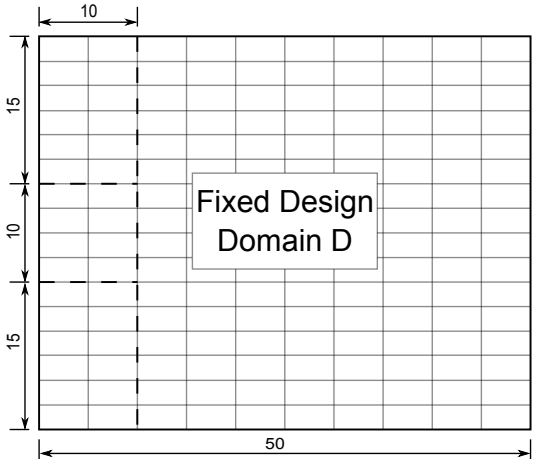

Figure 5: Fixed design domain discretization with the dimension of each component. Measures in millimeters.

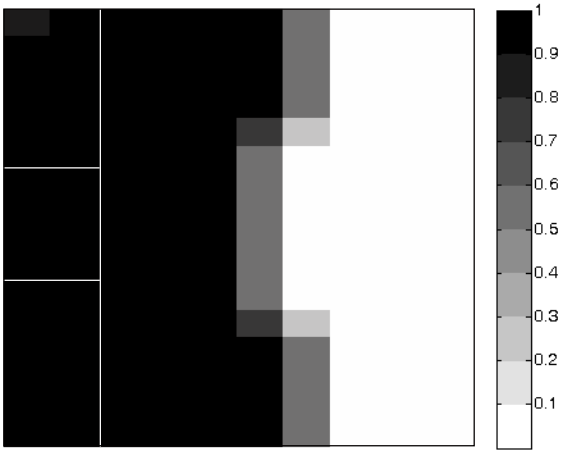

Figure 6: Optimal configuration to the graphite die.

Figure 6 shows the design variables of each finite element. Black regions represent the graphite die, white regions represents air, and gray regions the interface between them. Figure

7 shows the temperature distribution in the optimized graphite die. Although a projection technique is not used, no checkerboards emerged and a clear structural boundary, where the thermal radiation boundary conditions occur, is obtained. Figure 8 presents the convergence curves (Figure 8a) and the domain volume history (Figure 8b) during the optimization process.

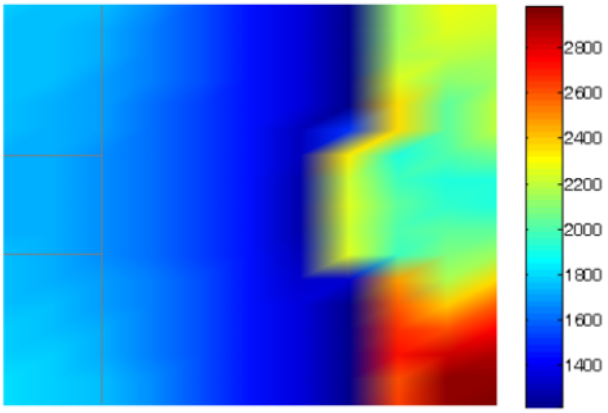

Figure 7: Temperature distribution provided by the optimized graphite die.

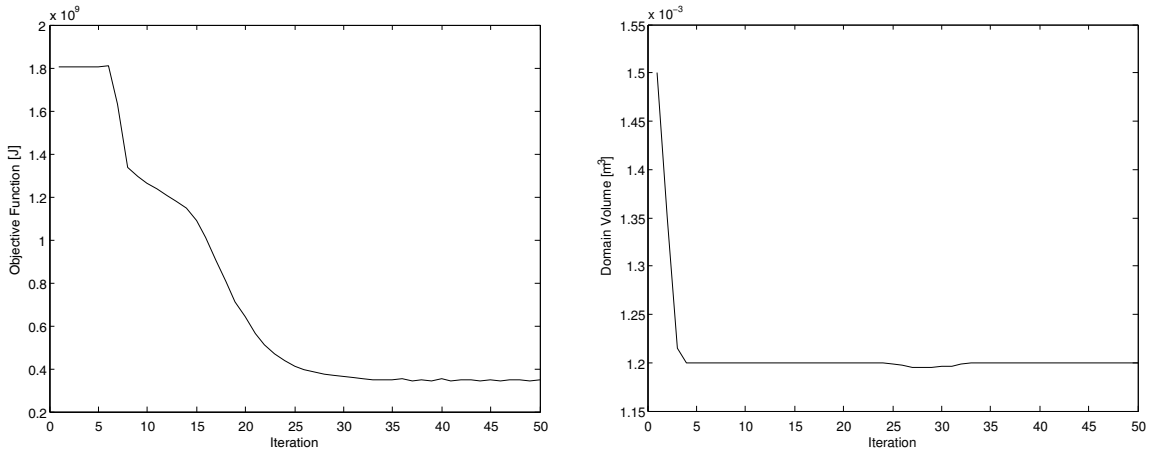

(a) (b)

Figure 8: (a) Convergence curve, (b) Domain volume history .

5 CONCLUSIONS

In this study, the topology optimization method is applied in the SPS process in order to obtain an optimized graphite die. COMSOL Multiphysics is used to perform a numerical simulation, from which the necessary information is obtained. The information is then used to compute proper boundary conditions, which are employed in the FE model.

The result shows that

1. There are no checkerboard instabilities in the optimized configuration.

2. A model based in the Hat-function to deal with design-dependent load is used to extract the structural boundary conditions and set the heat transfer boundary conditions.

3. A well defined 0 - 1 discretization and a uniform temperature distribuition are obtained, which confirms the FE formulation and the optimization algorithm.

4. The optimized configuration is obtained with relatively few iterations.

In a future work, we will consider other values of the weightening coefficient to optimize the temperature gradient in the sample. Related to the TOM, the projection technique will be used to avoid numerical instabilities when considering different material samples and temperature-dependent material properties. Finally, considering the temperature of the die surface equal to 1550K (see Figure 7), a temperature of linearization equal to 1750K, and the other values (such as the Stefan-Boltzmann coefficient) used in the paper, the linearization error is about 10% of the value of q_{rad} (Equation 5). This value is to be reduced by changing the linearization point.

ACKNOWLEDGMENTS

The second author thanks FAPESP for his postdoctoral scholarship (grant number 2009/18210-6). The third author acknowledges the financial support of the CNPq - grant number: 303689/2009-9. The first author acknowledges CAPES for providing him a master scholarship.

REFERENCES

Anselmi-Tamburini U., Gennari S., Garay J., and Munir Z. Fundamental investigations on the spark plasma sintering/synthesis process ii. modeling of current and temperature distributions. *Materials Science and Engineering*, A 394:139–148, 2005.

Bendsøe M. and Sigmund O. *Topology Optimization Theory, Methods and Applications*. Springer-Verlag, Germany, 2003.

Bruns T. Topology optimization of convection-dominated, steady-state heat transfer problems. *International Journal of Heat and Mass Transfer*, 50:2859–2873, 2007.

Gao T., Zhang W., Zhu J., Xu Y., and Bassir D. Topology optimization of heat conduction problem involving design-dependent heat load effect. *Finite Element in Analysis and Design*, 44:805–813, 2008.

Iga A., Nishiwaki S., Izui K., and Yoshimura M. Topology optimization of thermal conductors considering design-dependent effects, including heat conduction and convection. *International Journal of Heat and Mass Transfer*, 52:2721–2732, 2009.

Tiwari D., Basu B., and Biswas K. Simulation of thermal and electric field evolution during spark plasma sintering. *Ceramics International*, 35:699–708, 2009.

Vanmeensen K., Laptev A., Hennicke J., and der Biest O.V. Modelling of the temperature distribution during field assisted sintering. *Acta Materialia*, 53:4379–4388, 2005.

Wang X., Casolco S., Xu G., and Garay J. Finite element modeling of eletric current-activated sintering: The effect of coupled eletrical potential, temperature and stress. *Acta Materialia*, 55:3611–3622, 2007.

Yucheng W. and Zhengyi F. Study of temperature field in spark plasma sintering. *Materials Science and Engineering*, B90:34–37, 2002.

Zavaliangos A., Zhang J., Krammer M., and Groza J.R. Temperature evolution during field activated sintering. *Materials Science and Engineering*, A 379:218–228, 2004.